Using multicomponent seismic for reservoir characterization in Venezuela

Reinaldo J. Michelena, María S. Donati, Alejandro A. Valenciano, and Claudio D'Agosto, Petróleos de Venezuela (Pdvsa) Intevep, Caracas, Venezuela

This paper shows part of the effort in Venezuela during the last eight years to record, process, and interpret multicomponent seismic data. We present the main results of three projects aimed mainly to help other studies in fracture, lithology, and heavy oil characterization in different types of geologic environments.

Maporal Field. This field, in western Venezuela in the Barinas-Apure Basin, produces primarily from a fractured carbonate reservoir at a depth of 10 000 ft. The area is structurally simple. In early 1994, Pdvsa recorded in this field the first 3-C/2-D multicomponent survey in Venezuela to obtain information about fracture orientation and density at the reservoir level that could help design trajectories of horizontal wells.

The survey was designed to intersect existing well control and maximize data quality with respect to resolution and signal-to-noise ratio. Three 10-km 2-D multicomponent lines were centered over the reservoir along three azimuths. Lines 1 and 3 were parallel to the field's two main fault systems. Line 2 bisects the angle between lines 1 and 3, forming an angle of approximately 41° with line 1 (Figure 1). To avoid aliasing of surface waves, the geophone group interval was 17 m with a linear array between stations. The far offset was extended to 3600 m to allow converted-wave events to arrive outside the surface waves cone.

Figure 1 shows the behavior of migrated horizontal components around points 7 km from the beginning of each line. At the blue point on line 3, the radial component arrives faster than the transverse component. At the red point on line 1, the radial component arrives later. Similarly, at the green point on line 2, energy arrives faster in the transverse component. These observations suggest that the orientation of fast shear waves is roughly in the same direction of line 3, which is also parallel to the orientation of maximum horizontal stress.

We performed rotation analysis along the migrated horizontal com-

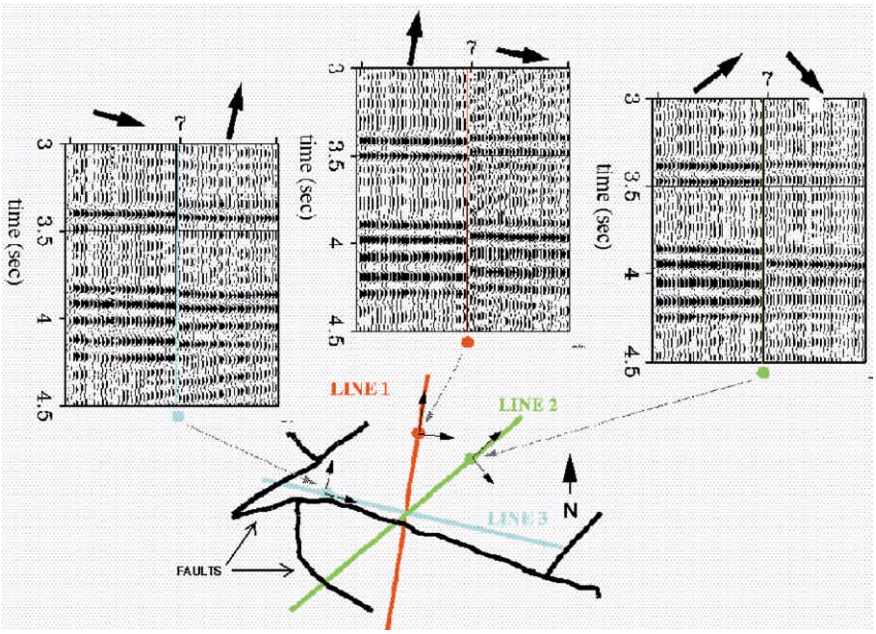

Figure 1. Examples of migrated horizontal components for selected locations along the 3-C lines. Rotation analysis of these data yielded the fracture orientation and density map in Figure 2.

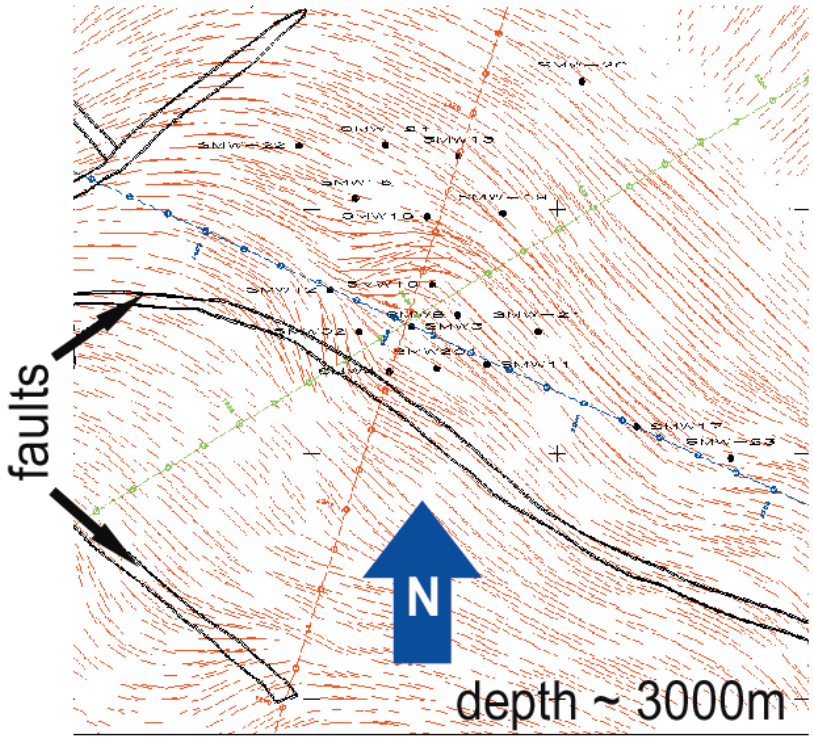

Figure 2. Map view of fracture orientation and density at the top of the carbonate reservoir. Maximum horizontal stress is parallel to line 3 (blue). Fracture orientations closely follow the alignment of major faults. Changes in fracture density are related to structural variations and changes in rock type.

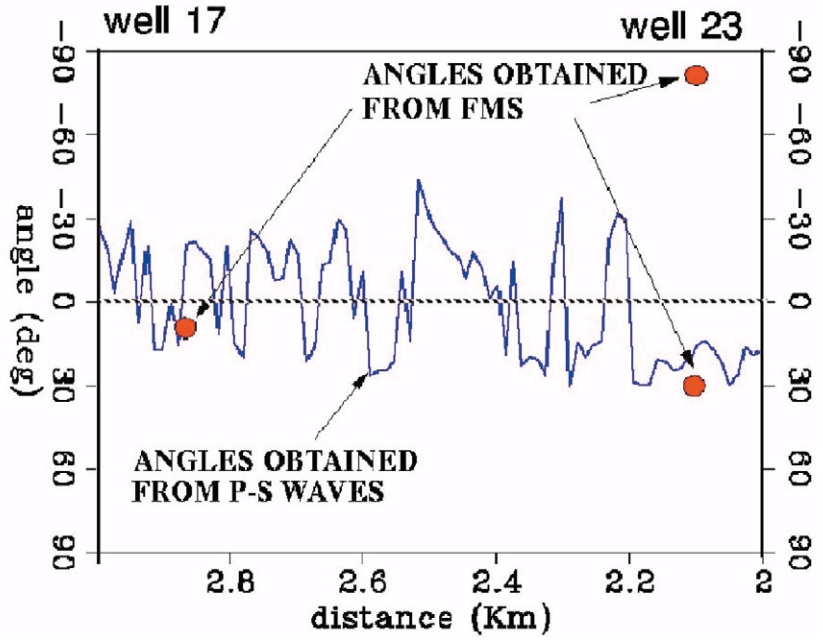

Figure 3. Comparison of fracture orientation from FMS logs and from multicomponent seismic data. Two fracture sets intersect well 23. Seismic data tend to follow the densest.

ponents to estimate the orientation of the faster shear arrival and the traveltime difference between the two arrivals at each point. The analysis was based on the ratios of amplitudes between the two horizontal components. After analyzing the energy ratios around various significant reflections, we obtained maps of orientation of the faster shear wave arrival which correlated very well the alignment of the major faults that cross the field. Figure 2 is a map generated at the top of the carbonate reservoir where the effect of upper layers has been removed by layer stripping. Orientations were estimated only along the 3-C lines. Angles for areas between lines were estimated by bidimensional splines interpolation. Lengths of red segments are proportional to differences in traveltime between fast and slow shear-wave arrivals. Figure 3 shows how orientations obtained from rotation analyses are also consistent with orientations obtained from FMS logs. They reveal that the dominant fracture system in the field strikes northwest-southeast, making an angle of approximately 30° with line 3. Because of the good correlation with the alignment of major faults in the field and the good agreement with the orientation of the dominant fracture set observed at the wells, we interpreted Figure 2 as the map of fracture orientation of the densest set of fractures in the field. This map was used to design trajectories of horizontal wells.

V_P/V_S ratio and lithology of formations right above the target are well correlated in this field. Figure 4 compares the V_P/V_S ratio estimated from a dipole sonic log with a gamma-ray log from the same well. V_P/V_S ratios obtained after a careful interpretation and correlation of *PP* and *PS* data follow the same trend of the V_P/V_S ratios obtained from the dipole sonic log. Ratios estimated from the seismic data are well correlated with net sand thickness estimated from gamma-ray logs at different locations. Seismic-derived V_P/V_S ratios were later used to generate maps of net sand thickness across the reservoir.

Figure 5 shows the relations among structural variations along line 1, changes in lithology indicated by changes in seismic-derived V_P/V_S ratio, and changes in anisotropy (proportional to fracture density) indicated by changes in traveltime differences between fast and slow shear-wave arrivals along the same line. The green line indicates the variations in depth of the top of the target. Notice how the intensity of anisotropy is not symmetric around the zone of the structure with strongest curvature. The reason for this asymmetry is because the flanks of the zone of strongest curvature contain different rock types that respond differently to the same deformation. Because shales are more plastic than sands, they tend to fracture less when a similar stress is applied to both.

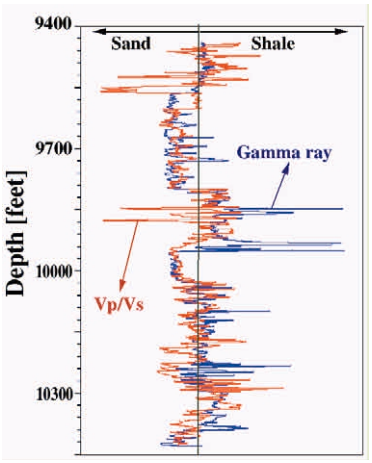

Figure 4. Correlation between gamma-ray log and V_P/V_S ratio.

Lagunillas Field. This field is east of Lake Maracaibo Basin. The target horizon is a Miocene Formation characterized by interbedded series of shales, clays, and highly unconsolidated sandstones at a depth of 2000-2600 ft (300-500 ms). Heavy oil serves as the "glue" that holds the rock together in the producing area. The reservoir is in a monocline structure with a mild dip to the southwest.

In 1997, Pdvsa recorded a 3-D/3-C baseline data set simultaneously with a conventional 3-D volume as part of a project to monitor steam injection. The purpose of the 3-D/3-C experiment was to evaluate the potential of using multicomponent data to quantify changes in reservoir conditions with time. Only the baseline survey has been recorded so far.

The 3-D/3-C survey covers 0.33 km^2. Sixteen geophones were permanently buried at a depth of 30 m; permanently burying the geophones ensures the required repeatability for a time-lapse study. Spacing between receivers and receiver lines was 196 m. The 4104 explosive sources were buried at a depth of 15 m and had a brick distribution. The same sources were used to acquire a conventional *P*-wave data set that covered a larger area. These *P*-wave data have good signal-to-noise ratio, high-frequency content, and good continuity along the target horizon.

The most significant results derived from processing this multicomponent survey were:

- Unconsolidated sands produce azimuthal anisotropy. As evident in Figure 6, there is coherent energy in both horizontal components along all time sections. We believe seismic data are responding in this case to

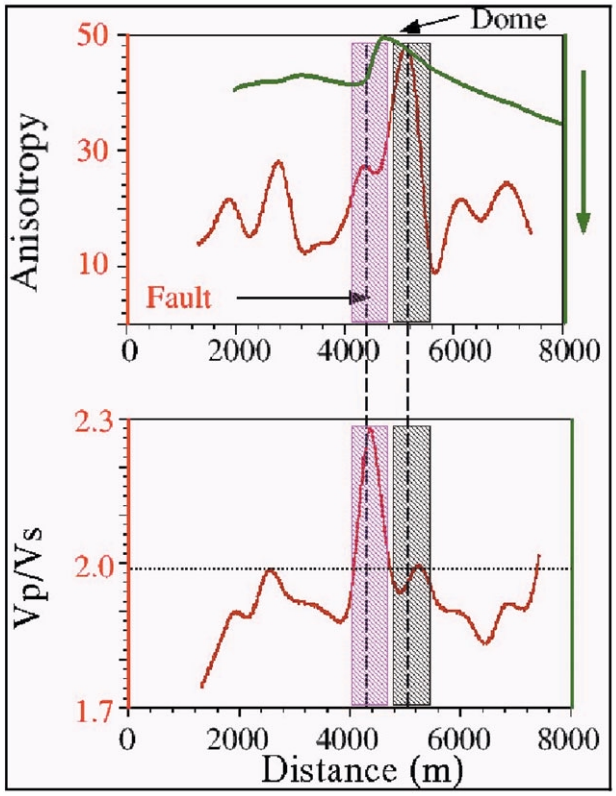

Figure 5. Relations among structural deformations, fracture density (proportional to strength of anisotropy), and lithology along line 1. The anisotropy vertical axis in the top figure indicates the difference in ms between fast and slow shear-wave arrivals. More plastic shales (V_P/V_S greater than 2, in pink) tend to fracture less than sands around the dome.

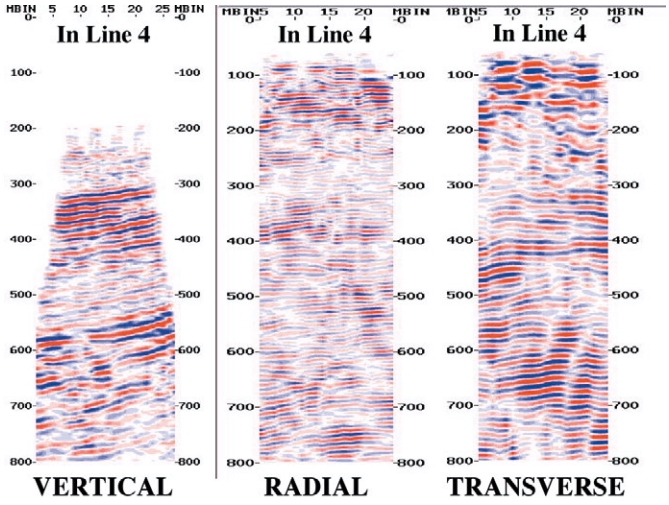

Figure 6. Time-migrated seismic sections for vertical, radial, and transverse component *PP* time. The energy in both horizontal components is clear evidence of azimuthal anisotropy in this field. The target is between 300 and 500 ms (*PP* time).

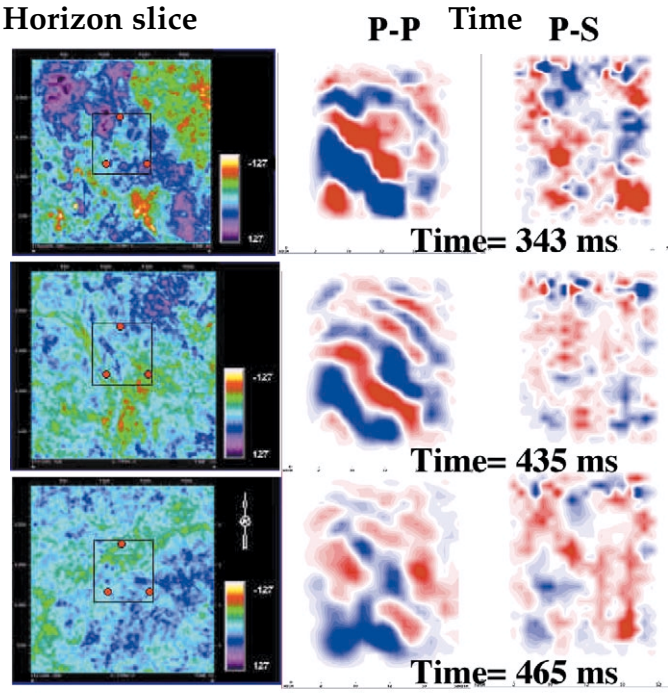

Figure 7. Comparison of horizon slices (from 3-D *P*-wave data) and times slices (from *PP* and *PS* seismic data). There is good correlation between both *P*-wave volumes. Strong changes in amplitude are observed in converted waves. The three red points are wells used in the processing.

the maximum horizontal stress in the area. No birefringence analysis has been performed so far in these data.

- Resolution of horizontal components is higher than resolution of vertical component (Figure 6), suggesting that much more detail about the reservoir can be obtained with *PS* data than with conventional *PP* data.
- Horizontal components show lateral variations in amplitude not observed in the vertical component. This can be seen in Figure 6 and more clearly in Figure 7, which compares three time slices of *PP* and *PS* data. The reasons for these changes are unknown but may be related to changes in reservoir conditions due to steam injected into the reservoir 18 months before the acquisition, lateral changes in azimuthal anisotropy, or lateral changes in lithology. Confirmation of any of the hypotheses will require more modeling and calibration and careful removal of azimuthal anisotropy effects.
- Time migrations using *PS* migration velocities yielded better images than migrations using *PS* rms velocities.

Orinoco Oil Belt. This area, the largest heavy oil accumulation in the world, is in Eastern Venezuela. Reservoirs consist of closely interbedded series of heavy-oil sand bodies at very shallow depths. In August 1997, one operator in the area recorded a 3-D/3-C multicomponent data set to test how 3-C data could help improve shallow resolution of reservoirs with little or no contrast of acoustic impedance between sands and shales. The 3-D/3-C data were processed by two contractors. This study uses one of their final *P-P* and *PS* migrated cubes. In addition to seismic data, Pdvsa was provided with dipole sonic, density, gamma-ray, and spontaneous potential logs from three wells (although not all logs were available for all wells).

Figure 8 shows how the gamma-

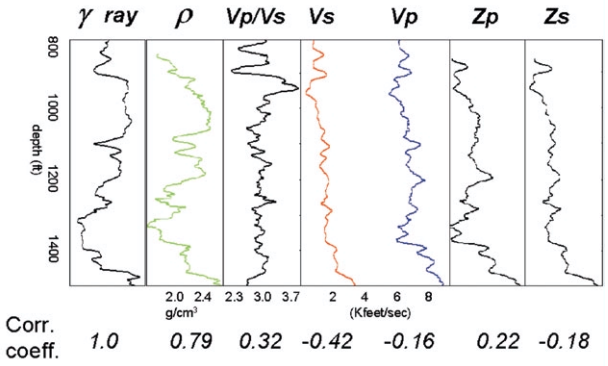

Figure 8. Correlations among gamma-ray, density, V_P/V_S ratio, *S*-wave velocity, *P*-wave velocity, *P*-wave impedance, and *S*-wave impedance logs. Numbers at the bottom are the correlation coefficients between gamma ray and the log above.

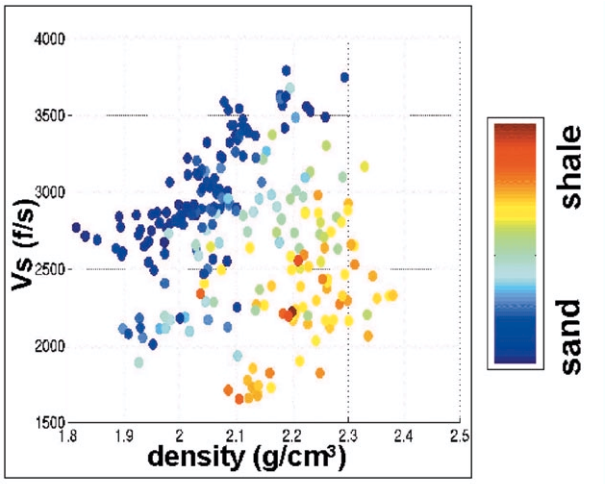

Figure 9. Plot of density versus *S*-wave velocity that is color-coded using the gamma-ray log. Sands and shales are clearly separated.

ray log correlates with different seismic properties such as velocities, densities, and impedances. As expected in this area, there is little correlation between gamma ray and acoustic impedance—the reason why compressional seismic data have not been reliable to detect changes in lithology. The correlation with wave velocities and lithology is also poor. The correlation with shear-wave velocities is better than with compressional-wave velocities. V_P/V_S and gamma ray are also poorly correlated. However, the correlation between gamma ray and density is high, which suggests that medium density can be used to help differentiate lithologies in this area. When the two parameters that show the highest correlation with gamma ray (density and shear-wave velocity) are crossplotted and each point is colored with the corresponding gamma-ray value, we observe better separation between sands and shales (Figure 9). This suggests that elastic parameters of the medium estimated from seismic data can be used to differentiate shales from sands after training a classification algorithm at the well.

An arbitrary line that intercepted the three wells where logs were available was extracted from the 3-D/3-C *PP* and *PS* cubes. We used a commercial algorithm to perform stratigraphic inversion of these two poststack lines. The results were combined to obtain the elastic parameters of the medium (Valenciano and Michelena, 2000). Figure 10 shows a density section obtained after inverting *PS* poststack data and combining this result with the acoustic impedance and estimates of the product

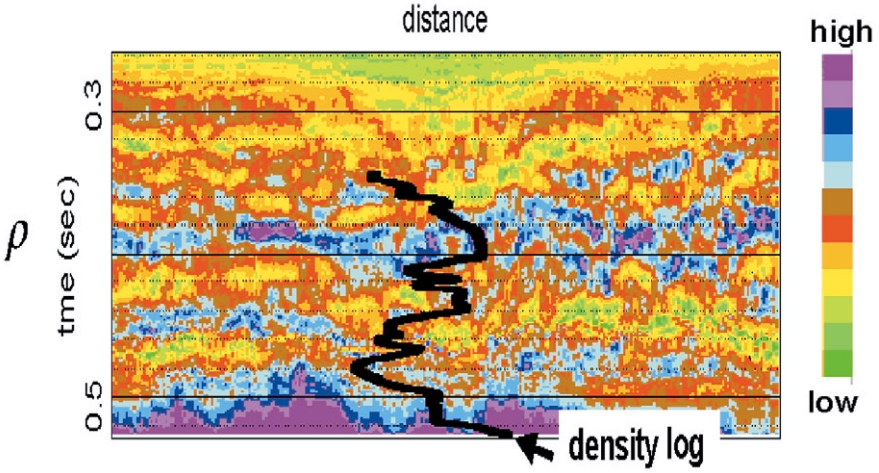

Figure 10. Density section estimated after combining *PP* and *PS* inversions. There is good agreement between estimated and expected densities except between 0.2 and 0.4 s, where the seismic derived density shows lateral variations around the well.

V_P/V_S and ratio V_P/V_S derived from the dipole sonic log.

Figure 11 shows the lithology distribution over the arbitrary line extracted from the 3-D/3-C data set. This was obtained after extrapolating along the section the relations between velocities and density at the well in the middle. The extrapolation of relations among elastic parameters was performed by using a neural-net-based classification algorithm on the elastic parameters derived from the seismic data. Sands are blue, shales are red, and transition zones are yellow.

These encouraging results helped justify the current reprocessing of these data with more emphasis on static corrections, wavelet processing, and preservation of true relative amplitudes.

Final remarks. Pdvsa faces many reservoir characterization challenges in Venezuela, particularly on land, in which multicomponent seismic can make enormous contributions. Many Venezuelan reservoirs have complex stratigraphy and are in structurally complex areas. Fracture, lithology, and fluids characterization in complex areas require better seismic images. For this reason, geophysicists in Pdvsa will focus in the next few years on the use and enhancement of 3-C seismic processing and imaging algorithms, and the development of new analysis/interpretation methods for these data. Particular emphasis will be on estimation of petrophysical parameters and interpretation of 3-C seismic attributes. As part of its exploration and production strategy, Pdvsa plans to use 3-C seismic to help

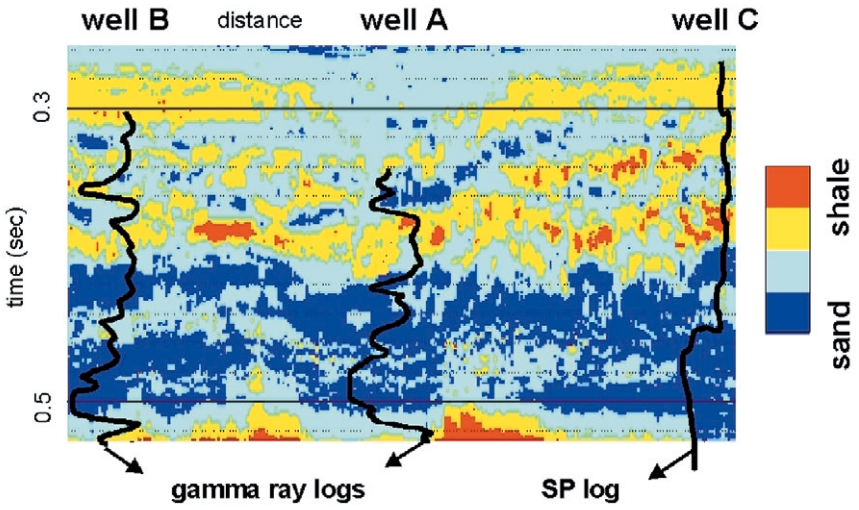

Figure 11. Lithology distribution after classifying the estimated elastic parameters using a neural-net-based algorithm. There is good agreement between seismic-based predictions and well logs, in particular below 0.44 s where the target is located. The initial model was built using only information from well A.

delineation and characterization of offshore reservoirs in the near future.

Suggested reading. "Multicomponent 3-D seismic pilot study in the Orinoco heavy oil belt," by Lansley et al. (*TLE*, 1998). "Mapping distribution of fractures in a reservoir with *PS* converted waves," by Ata and Michelena (*TLE*, 1995). "Birefringence study on 3-C/2-D: Barinas Basin (Venezuela)" by Donati and Brown (SEG 1995 *Expanded Abstracts*). "Quantifying errors in fracture orientations estimated from *PS* converted wave" by Michelena (SEG 1995 *Expanded Abstracts*). "Stratigraphic inversion of poststack *PS* converted waves data," by Valenciano and Michelena (SEG 2000 *Expanded Abstracts*). "Tomography + prestack depth migration of *PS* converted waves" by D'Agosto et al. (SEG 1998 *Expanded Abstracts*). "*P*- and *S*-wave separation at a liquid-solid interface," by Donati and Stewart (*Journal of Seismic Exploration*, 1996). "Making AVO analysis for converted waves a practical issue" by Donati and Martín (SEG 1998 *Expanded Abstracts*). E

Acknowledgments: This paper is the result of eight years of effort by many individuals within Pdvsa. Eulogio del Pino initially championed within Corpoven (a former affiliate of Pdvsa) using 3-C data to characterize fractures. Subsequently, many people have been involved in the different Pdvsa multicomponent projects. Elías Ata, Manuel González, Jesús Sierra, Javier Pérez, Rafael Banchs, Germán Pérez, Edgardo Padrón, Alberto La Cruz, Martin Carry, Mariangela Capello, Hermes Malcotti, Antonio Caldera, Carlota Pereira, and José Luis Pérez are just a few. Many results in this paper, and many more not shown, are in one way or another the result of their work. We processed the Lagunillas 3-C data using SeisUp from Geocenter Inc. Thanks also to Sincor for permission to present results from its area and to Pdvsa Intevep for permission to publish this paper.

Corresponding author: michelenar@pdvsa.com